N72-30918

NASA CONTRACTOR REPORT

NASA CR-2115

NASA CR-2115

CASE FILE COPY

A METHOD OF LIMIT POINT CALCULATION IN FINITE ELEMENT STRUCTURAL ANALYSIS

by R. H. Gallagher and S. T. Mau

Prepared by
CORNELL UNIVERSITY
Ithaca, N.Y.
for Langley Research Center

NATIONAL AERONAUTICS AND SPACE ADMINISTRATION • WASHINGTON, D. C. • SEPTEMBER 1972

1. Report No.	2. Government Accession No.	3. Recipient's Catalog No.
NASA CR-2115		

4. Title and Subtitle	5. Report Date
A METHOD OF LIMIT POINT CALCULATION IN FINITE ELEMENT STRUCTURAL ANALYSIS	September 1972
	6. Performing Organization Code
7. Author(s) R. H. Gallagher and S. T. Mau	8. Performing Organization Report No.
	10. Work Unit No. 134-14-05-02
9. Performing Organization Name and Address Cornell University Ithaca, NY	11. Contract or Grant No. NGL 33-010-070
	13. Type of Report and Period Covered Contractor Report
12. Sponsoring Agency Name and Address National Aeronautics and Space Administration Washington, DC 20546	14. Sponsoring Agency Code

15. Supplementary Notes

16. Abstract

An approach is presented for the calculation of limit points for structures described by discrete coordinates, and whose governing equations derive from finite element concepts. The nonlinear load-displacement path of the imperfect structure is first traced by use of a direct iteration scheme and the determinant of the governing algebraic equations is calculated at each solution point. The limit point is then established by extrapolation and imposition of the condition of zero slope of the plot of load vs. determinant. Three problems are solved in illustration of the approach and in comparison with alternative procedures and test data.

17. Key Words (Suggested by Author(s))	18. Distribution Statement
Finite element methods Nonlinear analysis Buckling Large displacements	Unclassified - Unlimited

19. Security Classif. (of this report)	20. Security Classif. (of this page)	21. No. of Pages	22. Price*
Unclassified	Unclassified	29	$3.00

*For sale by the National Technical Information Service, Springfield, Virginia 22151

TABLE OF CONTENTS

LIST OF SYMBOLS

$b_o, b_1 \ldots b_m$	Coefficients in the extrapolation formula of λ and Det.
$c_o, c_1 \ldots c_3$	Coefficients in the extrapolation formula of λ and Δ_s^k.
Det, Det_i	Determinant of the total stiffness matrix and determinant at the ith load level.
EA, EI	Axial and flexural rigidities, respectively.
$\lfloor f_e \rfloor$, f_{e_i}	Element displacement shape function vector and component.
[K], K_{ij}	System linear stiffness matrix and coefficients.
k_1, k_2, k_3	Spring constants of the non-linear foundation.
L	Total length of beam.
$[N_1(\Delta)], (N_2(\Delta^2)]$, N_{ijk}, $N_{ijk\ell}$	Structure geometric stiffness matrices and coefficients.
{P}, P_i	Structure nodal force vector and component.
w, w_o, $w_{o_{max}}$	Beam transverse displacement, initial value, and maximum initial value.
$\{\Delta\}$, Δ_i	Displacement vector and component.
Δ_j^i	Initial displacement component.
Δ_s^k	Amplitude of specified displacement component at load intensity λ^k.
Δ_s^u	Amplitude of specified displacement at limit load intensity, λ^u.
λ	Load intensity.
λ^c	Load intensity for bifurcation (knee-frame problem).
λ^u	Limit load intensity.
λ^q, λ^k	Load intensities at typical load levels q and k, respectively.
θ	Angular displacement of joint of knee-frame.

I. INTRODUCTION

Progress in the analysis of post-critical behavior of structures has recently been delineated by Bienek[1] and Hutchinson and Koiter[2]. One important class of problem described in these surveys concerns structures for which the slope of the postbuckling load versus displacement curve is negative. In such cases the imperfect actual structure may fail, or "snap-through" at a load intensity below bifurcation of the perfect form of the same structure. The objective of this report is to present an approach to the calculation of limit points for structures described by discrete coordinates and whose governing equations derive from finite element concepts.

Modern developments in limit point calculation have centered about the perturbation concepts pioneered by Koiter[3] and established in alternate form by Sewell[4] and Thompson[5]. Application of these concepts in the context of classical theory has expanded considerably the understanding of post-critical phenomena. This understanding has been broadened through the extension of finite element structural analysis procedures[6-10]. In finite element structural analysis, however, perturbation methods require extensive and complex algebraic operations. Additionally, although limitations of the applicability of such methods to linear prebuckling states have been removed,[9,10] they are intrinsically asymptotic procedures with validity limited to behavior close to bifurcation.

The method presented here takes the form of a simple computational algorithm and does not sustain the limitations of an asymptotic theory. First, the nonlinear load-displacement path of the imperfect structure is traced by use of an accelerated direct iteration scheme and the determinant of governing algebraic equations is calculated at each solution point. Then, by Lagrange interpolation, a functional representation of the load (λ) vs. determinant (Det.) behavior is constructed. The limit point is established by extrapolation and imposition of the condition of zero slope of the λ-Det. curve. In its present form the method does not allow for calculation of load-displacement response beyond the limit point.

Three problems are solved in illustration of the method and in verification of its accuracy. Although these are beam, arch, and frame structures the finite element concept is represented by the formulative basis of the elements employed in these analyses (assumed displacement fields) and by the form of the nonlinear algebraic equations under study. The present method is demonstrated to be accurate in all of the above cases. Experience in these and other numerical solutions allows conclusions to be drawn regarding selection of solution points and convergence.

II. ELEMENT AND SYSTEM FORMULATIONS

The purpose of this section is to define the general algebraic form of finite element stiffness equations for the present geometrically nonlinear analysis. The term "finite element stiffness equations" implies that the elastic deformational behavior of each designated region of the complete structure is to be characterized by certain displacement parameters, or degrees-of-freedom (d.o.f.), $\{\Delta\}$. The description of the displacement field (Δ) within the region of the structure is accomplished with use of shape functions $\lfloor f_e \rfloor$, so that

$$\Delta = \lfloor f_e \rfloor \{\Delta\} \tag{1}$$

or, in indicial notation, $\Delta = \lfloor f_{e_i} \Delta_i$. Indicial notation is especially useful in geometrically nonlinear finite element analysis and is employed in description of the developments to follow. Illustration of the detailed definition of these parameters and of the subsequent formulation of element relationships on that basis is given in Reference 11 for the case of a beam element on an elastic foundation.

The physical problem towards which the present work is directed is characterized by initial displacements due to fabricational inaccuracy. In accounting for these in the following we assume that the initial displacements are distributed throughout the structure in a form identical to the elastic displacements (Equation 1). Hence, the initial displacements are properly described by the joint values (indicial notation) Δ_j^i. Also, we designate the total displacements by Δ_j^T. Using these designations, the system stiffness equations for small strain non-incremental finite displacement analysis, for conservative loading and a Lagrangian frame of reference, are of the form[6]

$$K_{ij}\ (\Delta_j^T - \Delta_j^i) + N_{ijk}\Delta_j^T\ \Delta_k^T - N_{ijk}\ \Delta_j^i\ \Delta_k^i + N_{ijk\ell}\ \Delta_j^T\ \Delta_k^T\ \Delta_\ell^T$$
$$- N_{ijk\ell}\ \Delta_j^i\ \Delta_k^i\ \Delta_\ell^T - \lambda\ P_i = 0 \qquad (2)$$

where K_{ij} is the coefficient of the linear (small displacement theory) stiffness matrix [k].

N_{ijk} is the coefficient of the first-order nonlinear portion of the stiffness relationships.

$N_{ijk\ell}$ is the coefficient of the second-order nonlinear portion of the stiffness relationships.

P_i is a component of the applied load vector ({P}), in normalized form.

λ is the load parameter, a scalar, which can be adjusted to define a desired intensity of loading.

Noting now that the net displacements are $\Delta_j = \Delta_j^T - \Delta_j^i$, substituting this into Eq. (2) and collecting terms, we have the desired form of governing equilibrium equation

$$K_{ij}\ \Delta_j + N_{ijk}\ \Delta_j\ \Delta_k + N_{ijk\ell}\ \Delta_j\ \Delta_k\ \Delta_\ell$$
$$+ 2N_{ijk}\ \Delta_j^i\ \Delta_k + 3\ N_{ijk\ell}\Delta_j^i\Delta_k\Delta_\ell - \lambda P_i = 0 \qquad (3)$$

where only linear terms of Δ_j^i are retained.

III. SOLUTION OF EQUILIBRIUM EQUATIONS

The method chosen here for solution of the equilibrium relationship (Equation 3) is direct iteration. To describe this concisely it is useful to transform Equation 3 to matrix form, as follows

$$[K]\{\Delta\} + [N_1(\Delta)]\{\Delta\} + [N_2(\Delta^2)]\{\Delta\}$$
$$+ [2N_1(\Delta^i)]\ \{\Delta\} + [3N_2(\Delta^i,\Delta)]\{\Delta\} - \lambda\{P\} = 0 \qquad (3a)$$

where now $[N_1(\Delta)]\{\Delta\}$ and $[N_2(\Delta)^2]\{\Delta\}$ are formed from $N_{ijk}\Delta_j\ \Delta_k$ and $N_{ijk\ell}\ \Delta_j\Delta_k\Delta_\ell$, respectively, and $[2N_1(\Delta^i)]\{\Delta\}$ and $[3N_2(\Delta^i,\Delta)]\{\Delta\}$ are formed from $2N_{ijk}\ \Delta^i_j$ and $3N_{ijk\ell}\Delta^i_j\Delta\Delta$, respectively.

In the basic form of the iterative method it is assumed that the solution is to be obtained for a load intensity λ^q, and that solution data from a prior load level, say λ^{q-1}, is available and designated as $\{\Delta\}^o$. Thus, the matrices $[N_1(\Delta)^o]$, $[N_2(\Delta,\Delta)^o]$, $[2N_1(\Delta^i)^o]$ and $[3N_2(\Delta^i,\Delta)^o]$ may be formed using $\{\Delta\}^o$ and we may solve Equation (3a) to yield

$$\{\Delta\}^1 = [k]^{-1}\{\lambda^q\{P\} - [N_1(\Delta)^o]\{\Delta\}^o - [N_2(\Delta,\Delta)^o]\{\Delta\}^o$$
$$- [2N_1(\Delta^i)]\{\Delta\}^o - [3N_2(\Delta^i,\Delta)^o]\{\Delta\}^o\} \qquad (4)$$

where the superscript 1 on $\{\Delta\}^1$ denotes the first iteration in the solution at λ^q. We then re-form $[N_1(\Delta)]$, etc. on the basis of $\{\Delta\}^1$, so that

$$\{\Delta\}^2 = [K]^{-1}\{\lambda^q\{P\} - [N_1(\Delta)^1]\{\Delta\}^1 - N_2(\Delta,\Delta)^1]\{\Delta\}^1$$
$$- [2N_1(\Delta^i)]\{\Delta\}^1 - [3N_2(\Delta^i,\Delta)^1]\{\Delta\}^1\} \qquad (5)$$

which is now solved for $\{\Delta\}^2$. In the general, j^{th}, iterative solution is

$$\{\Delta\}^j = [K]^{-1}\{\lambda^q\{P\} - [[N_1(\Delta)^{j-1}] + [N_2(\Delta,\Delta)^{j-1}]$$
$$+ [2N_1(\Delta^i)] + [3N_2(\Delta^i,\Delta)^{j-1}]]\{\Delta\}^1\} \qquad (6)$$

The iterative sequence continues until $\{\Delta\}^j$ is within $\{\Delta\}^{j-1}$ to a specified tolerance. Note that direct iteration requires only the inversion of the linear stiffness matrix and continued re-formation of $[N_1(\Delta)]$, etc.

The knowledge of a nearby solution, as for $\{\Delta\}^o$ in Equation (4), enhances the efficiency of the iterative process. Hence, the analysis is performed at various load levels, from a level close to zero to a level as close as possible to limit load. Convergence difficulties are encountered when the nonlinearities are severe. In such cases an improved procedure is to employ a higher-order iterative scheme as described in Reference 11.

IV. EXTRAPOLATION FOR CALCULATION OF LIMIT POINT

According to the energy criterion of stability(2), the limit point is characterized by the vanishing of the second variation of the total potential energy of the structure. In a finite element formulation the corresponding criterion is that the determinant of the total stiffness matrix is zero. Thus, it is not possible to accomplish the solution of Equation 3a at the limit point. The evaluation of the load and displacement at this point is accomplished by extrapolation of determinants of solutions at prior points on the pre-buckling path, as described in the following, and illustrated in Figures 1 and 2.

We designate by the symbol (Det) the determinant of the equilibrium equations 3a, i.e.

$$\text{Det.} = |K_j + 2N_1(\Delta) + 3N_2(\Delta,\Delta) + 2N_1(\Delta^i) + 6N_2(\Delta^i,\Delta)| \tag{7}$$

As indicated above, the determinant of the total stiffness matrix is zero at the limit point and in addition (see Figure 2) there is a stationary point on the λ-Det relationship, i.e.

$$\left.\frac{d\lambda}{d(\text{Det})}\right|_{\lambda=\lambda^u} = 0 \tag{8}$$

where λ^u designates the intensity of the loading parameter at limit load.

A series representation of λ versus Det may be written in the form

$$\lambda = b_o + b_1 \text{ (Det)} + b_2 \text{ (Det)}^2 + \ldots + b_m \text{ (Det)}^m \quad (9)$$

where m is the number of fundamental-path solution points employed and $b_o \ldots b_m$ are coefficients to be determined. By application of Equation (8), $b_1 = 0$. Then, a system of simultaneous equations for calculation of b_o, b_2, ... b_m is established by evaluation of Equation (9) at each of the m points. E.g., at the typical point k on the fundamental path

$$\lambda^k = b_o + b_2 \text{ (Det)}_k{}^2 + \ldots b_m \text{ (Det)}_k{}^m \quad (10)$$

This yields a system of m equations whose solution furnishes the coefficients b_o, b_2, ... b_m. The limit point is computed by setting Det to zero in Equation (9). Thus, at the limit point, $\lambda^u = b_o$.

It should be noted that at least three terms are needed in Equation 10. This expression is equivalent to a Taylor series expansion about the limit point. Since the first derivative is zero at that point the linear term does not appear and at least the $(\text{Det})^2$ term should be included. If only the $(\text{Det})^2$ is included, however, the resulting curve is a parabola symmetric about the limit point. To cope with skewness in the curve, which is likely to exist, the $(\text{Det})^3$ term should be included.

No rules can be suggested for the best number of terms beyond three. Equation 10 represents extrapolation for which error estimation is not possible. In practice, the number of terms is limited by the number of load levels used in the pre-buckling calculation, which in turn depends on the scheme used to generate the next load level. The scheme used here in ullustrative examples is to choose the load level at the 1/3 point between the prior load level and the estimated limit load.

The extrapolation to determine the displacement at the limit point differs from the extrapolation to determine the limit load in that a fixed number of solution points is employed and the value of the limit load is also used. First, the load parameter-displacement relationship is assumed to be of cubic form

$$\lambda^k = c_o + c_1 \Delta_s^k + c_2(\Delta_s^k)^2 + c_3 (\Delta_s^k)^3 \qquad (11)$$

where c_o, c_1, c_2 and c_3 are constants to be determined and Δ_s^k is the displacement in the specified degree-of-freedoms evaluated at the load intensity λ^k. Equation 11 is constructed for each of three load intensities. Also, evaluation at the limit point ($\lambda^k = \lambda^u$, $\Delta_s^k = \Delta_s^u$) is accomplished

$$\lambda^u = c_o + c_1 \Delta_s^u + c_2 (\Delta_s^u)^2 + c_3(\Delta_s^u)^3 \qquad (12)$$

and it is noted that for this equation, Δ_s^u is as yet unknown. Finally, we have the condition at the limit point.

$$\left.\frac{d\lambda}{d\Delta}\right|_{\lambda=\lambda^u} = 0 \qquad (13)$$

and, by application to Equation 11

$$0 = c_1 + 2c_2 (\Delta_s^u) + 3c_3 (\Delta_s^u)^2 \qquad (14)$$

Thus, five nonlinear algebraic equations (three forms of (11), and (12) and (13)) are available for calculation of c_o, c_1, c_2, c_3 and Δ_s^u. It is convenient to accomplish this determination by eliminating three parameters by solution of the three linear equations (Eqs. 11), substitution of the result into (12) and (14), and solution of the latter by Newton-Raphson iteration. If the full vector of joint displacements is needed the above operation must be repeated for each degree-of-freedom.

The reasoning in selection of a third-degree polynomial in Equation (11) is as follows. This equation, like Equation (10), is equivalent to a Taylor series expansion about the limit point. *By the same argument as given above, no* less than a third-degree polynomial should be chosen. In the present case, since λ^u is already known and Equation (11) is used only to calculate the displacements at λ^u and not to give accurate predictions beyond the immediate vicinity of λ^u, higher order terms are not needed.

V. ILLUSTRATIVE EXAMPLES

1. Beam on Nonlinear Foundation

The purpose of this example, the axially-loaded beam on nonlinear elastic foundation shown in Figure 3, is the comparison of results obtained with the present method with results obtained by use of the perturbation method of Reference 10.

The nonlinear foundation modulus for the beam is given by $k_1w - k_2w^2 - k_3w^3$, where w is the transverse displacement and k_1, k_2, and k_3 are spring constants. k_1 simulates the linear stiffness [k]; k_2 and k_3 yield matrix coefficients which correspond to the $[n_1]$ and $[n_2]$ geometric stiffness matrices, respectively. Five different combinations of these constants were employed for the subject numerical solutions, as follows:

CASE	$k_1/EI/L^4$	$k_2/EI/L^5$	$k_3/EI/L^6$	$P_{cr}/EI/L^2$
I	16	0	16000	11.49
II	160	0	80000	26.09
III	16	500	0	11.49
IV	16	500	-1000	11.49
V	16	500	1000	11.49

In Cases I-III either k_2 or k_3 is set equal to zero to simulate cases where $[n_1]$ and $[n_2]$, respectively, are zero. Cases IV and V correspond to the general nonlinear finite element formulation of a non-symmetric structure. The above listing also gives the critical loads for the beam on linear elastic foundation as found in Reference 12.

In each Case the initial deviation of the complete beam is assumed to be of the form $w_o = w_{o_{max}} \sin \frac{\pi x}{L}$, where $w_{o_{max}}$ takes on values .01L, .02L, .03L, .05L, .06L, .07L, .08L, .09L, .10L. The finite element idealization consists of eight equal-length elements. Formulation of the pertinent element is detailed in Reference 11.

In the presence of imperfection, the axially loaded beam exhibits a snap-through type of buckling due to the continuously weakening foundation modulus $k_1 w - k_2 w^2 - k_3 w^3$. Figure 3 shows the foundation modulus for Cases I-III. A typical load-displacement plot is shown in Figure 4 for Case IV for values of $w_{o_{max}}$ of 0 and .01, demonstrating the nature of this effect.

Curves of limit points vs. the imperfection amplitude $w_{o_{max}}$ are plotted in Figure 5 for Cases I-III and in Figure 6 for Cases IV and V. Close agreement between the results of the present method and the perturbation approach is observed. The numerical results, summarized in Table I, show a 5% maximum discrepancy with solutions obtained using the perturbation method.

2. Hinged Circular Arch Under Central Point Load

This structure, shown in Figure 7, exhibits a highly nonlinear load-displacement path leading to snap-through buckling. An exact analytical solution, under the assumption of axial inextensibility, was published by Biezeno.[13] Haftka, et al[9] develop solutions by means of both the perturbation method and the so-called "modified structure" method, using finite element idealization consisting of straight axial-flexure elements. Experimental data and further theoretical work on this class of problem was recently reported by Dickie and Broughton[14].

Table 2 lists the solution points on the equilibrium path as calculated by the present iterative method. These results are plotted in Figure 7. In order to test the accuracy and convergence of the present approach to the prediction of the limit point load, extrapolations were carried out at different stages in the definition of the prebuckling path. The first attempt was made at solution point 3, using the data from points 1, 2 and 3. Calculations were then made at each succeeding solution point, using all prior points in defining the curve to be extrapolated. It is seen that an acceptable prediction (<5% error) is obtained when the final solution point is less than 70% of the limit point exact solution of Ref. (13). The solution is nearly exact for extrapolation from the point at 92% of the exact load level. It should be noted that the present analytical model includes the axial deformation so that the convergent solution is slightly different from that given in Reference 13.

Predictions of the central displacement (Δ_c) of the arch at the limit point were obtained for succeeding points in the manner described in Section IV. These results, expressed as a percentage of the Reference 13 solution, are listed in Table 2. The results are comparable in accuracy with the limit point load results and are quite acceptable at or beyond the 92% point.

The existence of an exact solution beyond the limit point enables assessment of the value of extrapolation in the post-buckling regime. The above (cubic-based) displacement curves were extended as shown in Figure 8. It is seen that reliable results beyond the limit point cannot be obtained by simple extrapolation.

3. Knee-Frame

The knee frame shown in Figure 9 was analyzed by Koiter[15] using his perturbation method and Roorda[16] has conducted tests of the same structure. The test data shown in this figure exhibit a snap-through buckling phenomenon due to the axial shortening of the column and the inherent imperfection of the thin strip member used in the test. If these factors are neglected, then the linear prebuckling analysis as performed in Reference 16 yields a bifurcation load $\lambda^c = 13.886 \frac{EI}{L^2}$.

The presentation of test data in Ref. 16 does not make clear if the value of λ^c in the ordinate λ/λ^c is a calculated or tested value. Haftka, et al[9] analyze the same frame using the "modified structure" method and employ for λ^c in this representation the value 14.022 EI/L^2, found by putting the vertical load slightly eccentric to the top of the column such that the resulting rotation at the joint of beam and column was negligibly small. Then, the load was placed $0.5 \times 10^{-4}L$ to the right of that neutral point to produce the curve shown in Figure 9; although the exact eccentricity of the neutral point is not defined.

In the present work the results shown in Figure 9 correspond to a vertical load acting at the top of the column and the snap-through is due to the axial shortening only. The normalizing λ^c is taken to be 13.668 EI/L^2, which is found by placing the load, after several trials $0.18 \times 10^{-5}L$ to the right of the top of the column to produce negligibly small rotations ($<0.5 \times 10^{-4}$ degrees) at the joint of beam and column. The extrapolated limit point, $\lambda^u = 13.525$ so that $\lambda^u/\lambda^c = 0.99$ is in close agreement with Roorda's test data. The last load level is $\lambda/\lambda^c = 12.6/13.668 = 0.92$.

VI. CONCLUDING REMARKS

A computationally-simple approach to the calculation of limit points has been presented and verified through comparison with prominent alternative solutions and test data. The most questionable aspect of this approach appears to be the use of extrapolation in prediction of both the limit load and the associated displacements. No difficulties were encountered from this source, however, in performance of the presented numerical analyses.

The basic limitation of the present method is due to the nature of extrapolation, namely error estimation is lacking. Although an extrapolated λ-u curve cannot be regarded as an accurate post-buckling curve, it is certainly a good "initial predictor" for a point beyond the limit point.

Certain investigations may require the tracing of the load-displacement path beyond the limit point. This initial predictor can be efficiently utilized when coupled with some other schemes for post-buckling analysis. Another way of accomplishing this is by initiation of analysis at the limit point and with decrementation of the loading. Other procedures appear promising and are under study.

REFERENCES

1. Bienek, M., "Post-Critical Behavior", Introductory Report for Ninth Congress of IABSE, Amsterdam, May, 1972.

2. Hutchinson, J. W. and Koiter, W. T., "Postbuckling Theory", Applied Mech. Reviews, V. 23, Dec. 1970, pp. 1353-1366.

3. Koiter, W. T., "On the Stability of Elastic Equilibrium", Thesis, Delft, 1945. Translation published as AFFDL-TR-70-25, Feb. 1970.

4. Sewell, M. J., "A General Theory of Equilibrium Paths Through Critical Points. I", Proc. Royal Soc. Ser. A, V. 306, pp. 201-223, 1968.

5. Thompson, J. M. T., "A General Theory for the Equilibrium and Stability of Discrete Conservative Systems" ZAMP, Vol. 20, 1969.

6. Morin, N., "Nonlinear Analysis of Thin Shells", Report R70-43, Dept. of Civil Engrg., M.I.T., 1970.

7. Lang, T. E., "Post-Buckling Response of Structures Using the Finite Element Method", Ph.D. Thesis, Univ. of Washington, 1969.

8. Walker, A. C., "A Nonlinear Finite Element Analysis of Shallow Circular Arches", Int. J. Solids Struct., V. 5, pp. 97-107, 1969.

9. Haftka, R. T., Mallett, R. H. and Nachbar, W., "A Koiter-Type Method for Finite Element Analysis of Nonlinear Structural Behavior", AFFDL TR 70-130, V. 1, Nov. 1970.

10. Gallagher, R. H., Lien, S. and Mau, S-T., "A Procedure for Finite Element Plate and Shell Pre- and Post-Buckling Analysis", Proc. of Third Conf. on Matrix Methods in Struct. Mech., Dayton, O., Oct. 1971.

11. Mau, S-T. and Gallagher, R. H., "A Finite Element Procedure for Nonlinear Pre-Buckling and Initial Post-Buckling Analysis", NASA CR-1936, January 1972.

12. Timoshenko, S. and Gere, J., "Theory of Elastic Stability", 2nd Ed., McGraw-Hill Book Co., 1961, pg. 94.

13. Biezeno, C. and Grammel, R., "Engineering Dynamics", V. 2. R. Blackie and Sons, Ltd., London, 1956.

14. Dickie, J. and Broughton, P., "Stability Criteria for Shallow Arches", Proc. ASCE, J. of the Eng. Mech. Div., V. 97, No. EM3, June 1971.

15. Koiter, W. T., "Post-Buckling Analysis of a Simple Two-Bar Frame", Recent Progress in Applied Mech. Broberg, et al, Ed. Almquist and Wiksell Publ., Stockholm, 1966.

16. Roorda, J., "Stability of Structures with Small Imperfections", Proc. ASCE, J. of Engrg. Mech. Div., V. 91, No. EM1, 1965.

TABLE 1: BEAM ON NONLINEAR ELASTIC FOUNDATION. VALUES OF NORMALIZED LIMIT POINTS (λ^u/λ^c) VERSUS $w_{o_{max}}$

		$w_{o_{max}}$									
	*	0	.01L	.02L	.03L	.05L	.06L	.07L	.08L	.09L	.10L
I	a	1	0.679	0.553	0.475	0.375	0.338	0.308	0.287	0.263	0.248
	b	1	0.680	0.555	0.475	0.372	0.336	0.308	0.284	0.263	0.243
II	a	1	0.599	0.470	0.384	0.291	0.256	0.236	0.216	0.198	0.182
	b	1	0.611	0.477	0.395	0.297	0.264	0.239	0.218	0.200	0.185
III	a	1	0.679	0.571	0.510	0.423	0.389	0.368	0.343	0.325	0.307
	b	1	0.680	0.582	0.517	0.431	0.399	0.374	0.351	0.332	0.313
IV	a	1	0.665	0.556	0.495	0.403	0.354	0.347	0.325	0.305	0.287
	b	1	0.669	0.566	0.499	0.410	0.379	0.353	0.329	0.309	0.291
V	a	1	0.695	0.588	0.537	0.455	0.428	0.388	0.384	0.363	0.348
	b	1	0.690	0.598	0.538	0.460	0.431	0.407	0.387	0.368	0.352

*SOLUTION PROCEDURES:

a: Extrapolation Method (present report)

b: Perturbation Method (Reference 11).

TABLE 2

HINGED SHALLOW ARCH PROBLEM - RESULTS OF EXTRAPOLATIONS FROM RESPECTIVE SOLUTION POINTS

Solution Points	Load Level* λ/λ_e	Extrap.Limit Load λ^u/λ_e	Extrap.Central Defl.** Δ_c/Δ_e
1	0	-	-
2	.230	-	-
3	.460	0.865	-
4	.690	0.965	0.895
5	.920	0.999	0.963
6	.935	1.002	0.984
7	.948	1.004	0.990
8	.971	1.007	1.004
9	.982	1.004	0.987
10	.990	1.006	1.002
11	.994	1.007	1.009

* λ_e - Exact limit load, from Ref. 13 = 432 lb.

** Δ_e - Exact value of central deflection from Ref. 13.

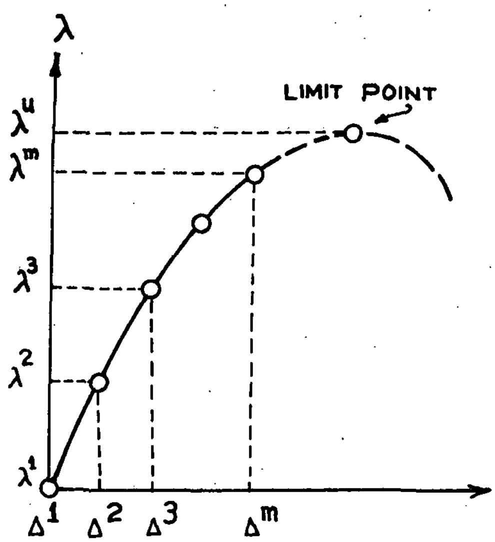

1. Representative Load-Displacement Plot.

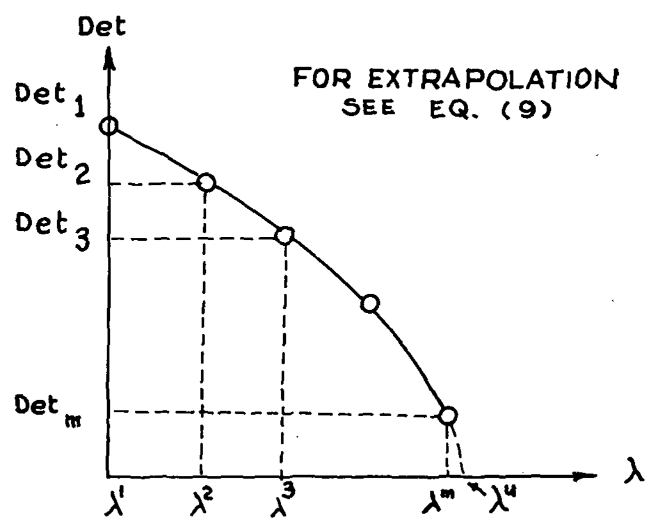

2. Determination of Limit Point via Extrapolation.

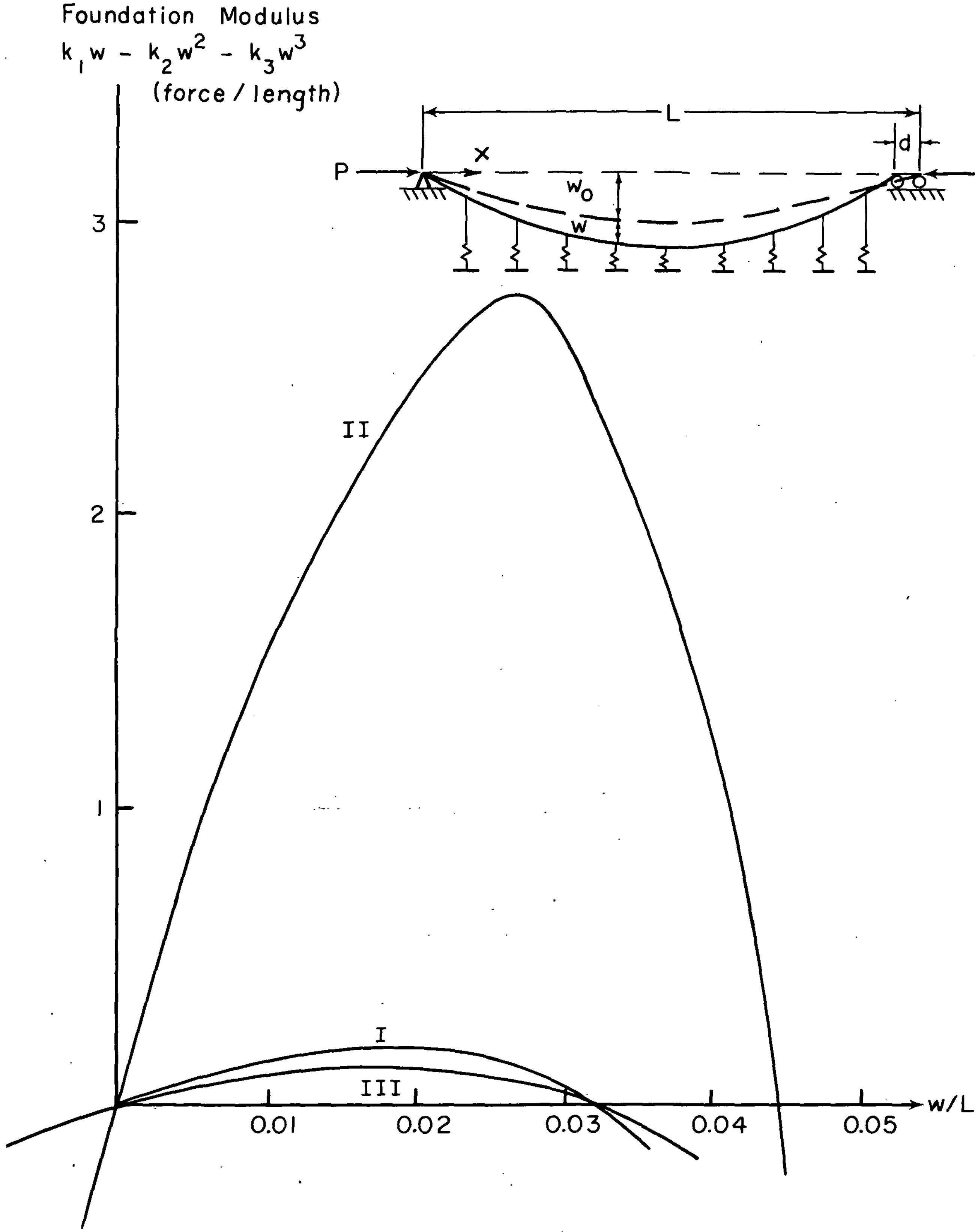

3. Foundation Properties. Beam on Nonlinear Elastic Foundation.

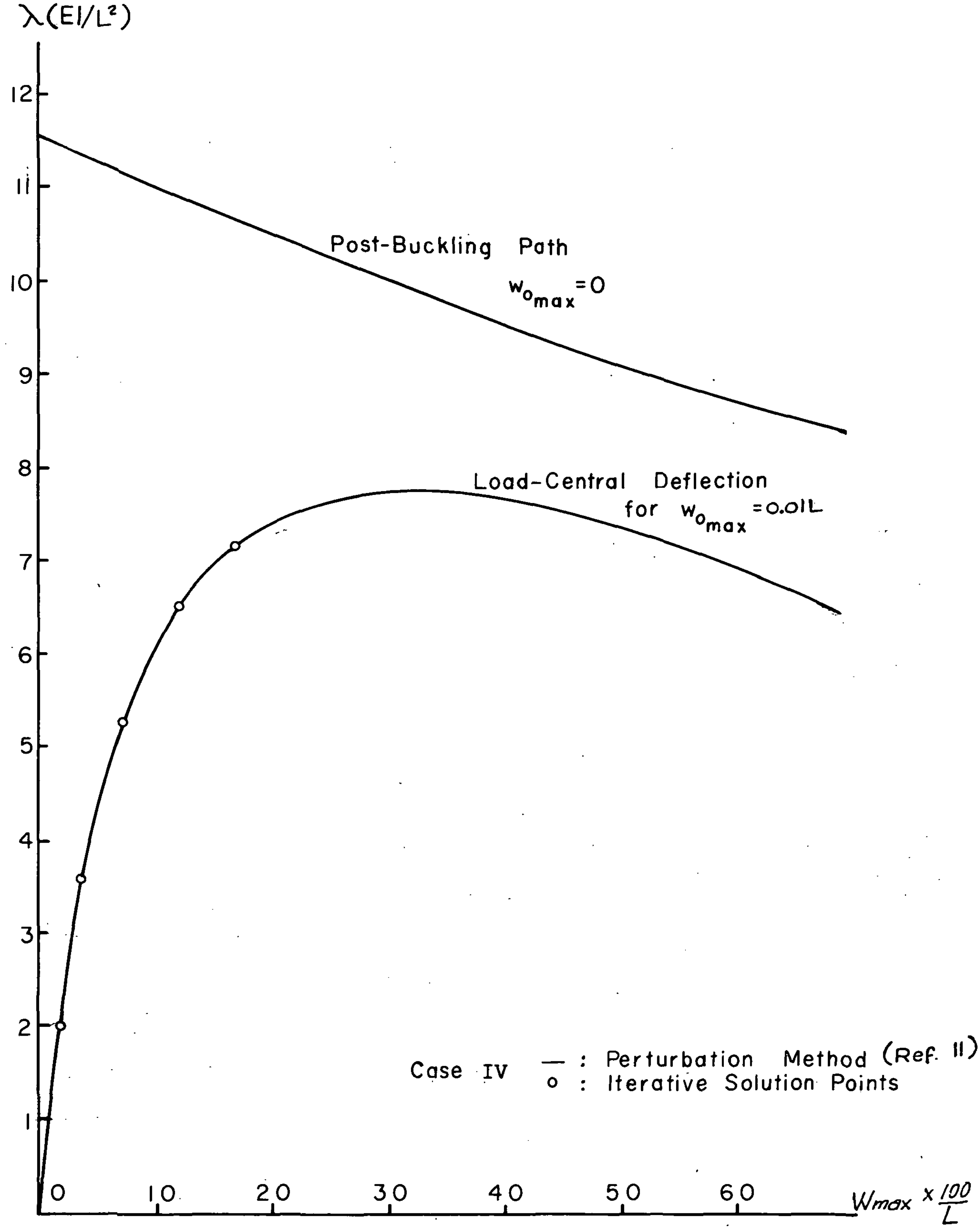

4. Beam on Nonlinear Elastic Foundation. Post-Buckling Path and Load-Displacement Relationship. Case IV.

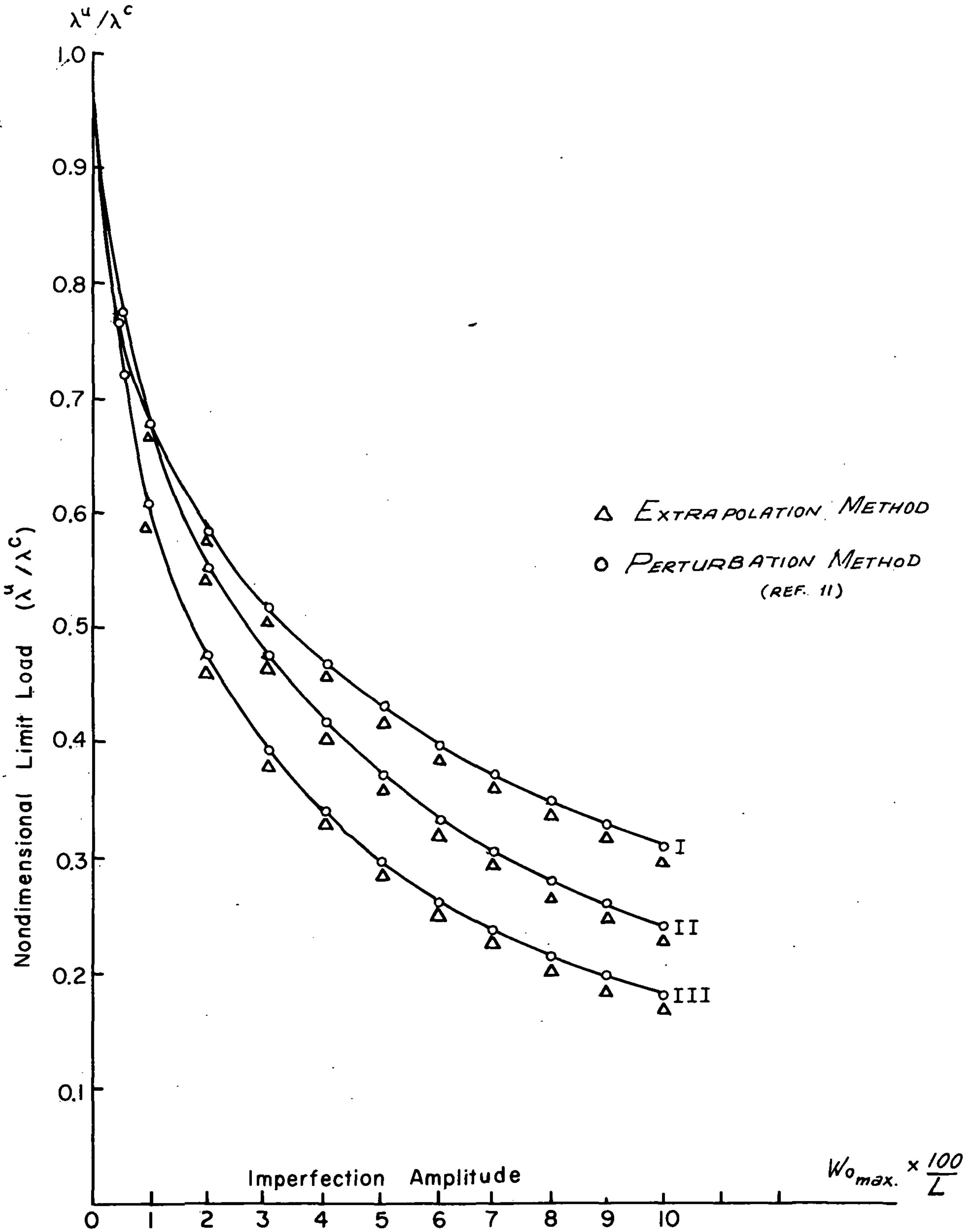

5. Beam on Nonlinear Elastic Foundation Limit Load as a Function of $w_{o_{max}}$. Cases I-III.

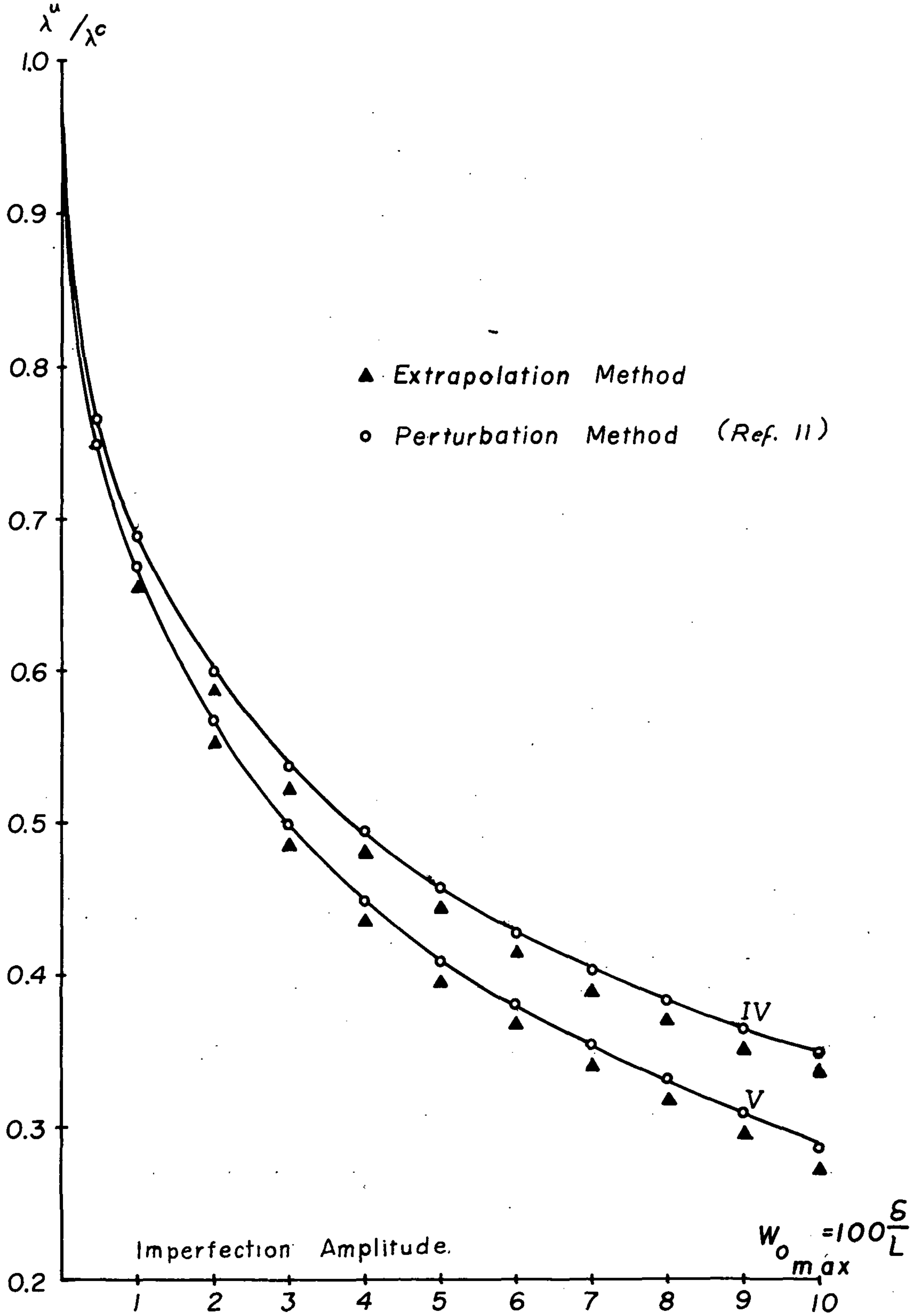

6. Beam on Nonlinear Elastic Foundation. Limit Load as a Function of $w_{o_{max}}$. Cases IV-V.

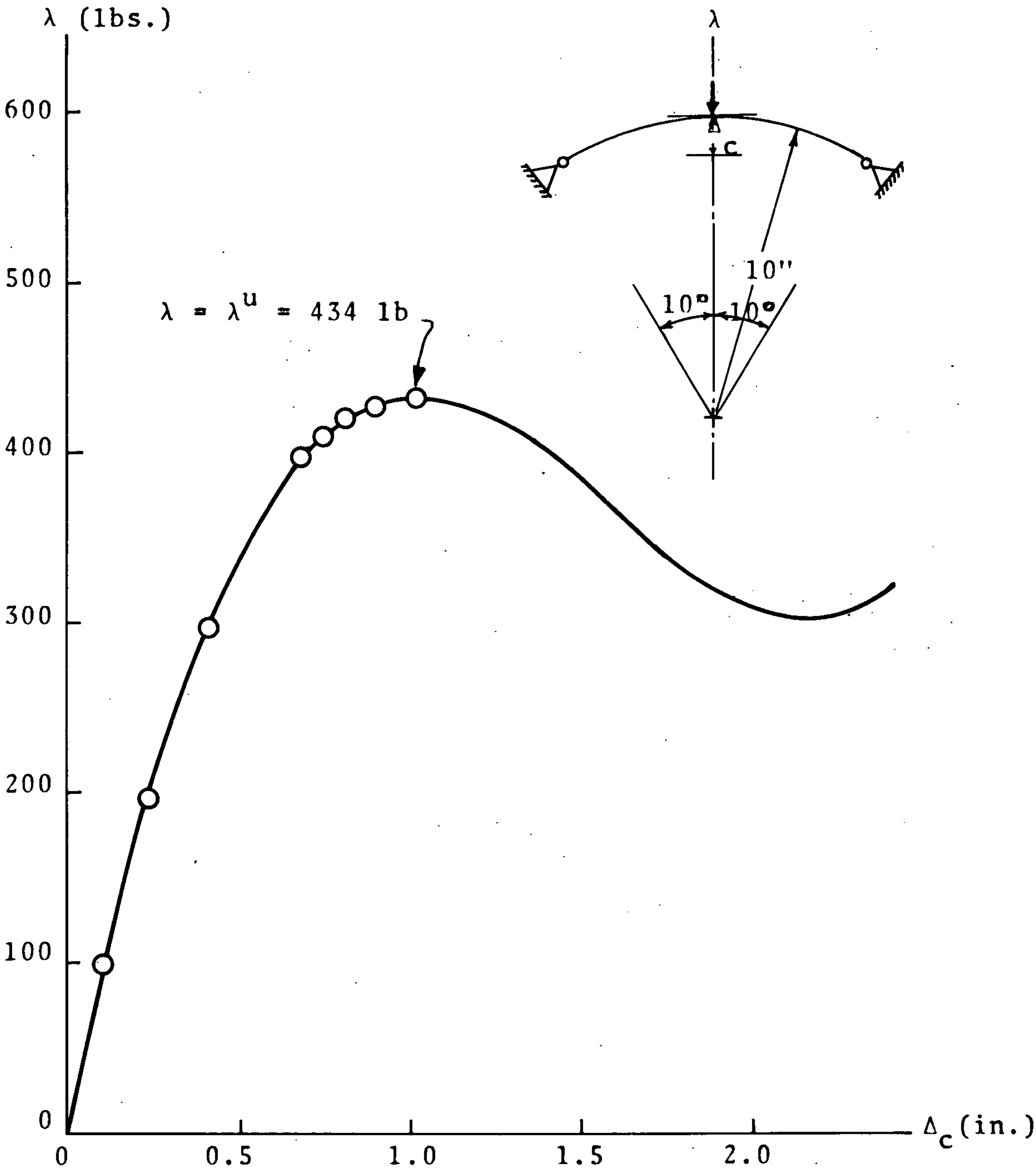

7. Load-Displacement Behavior of Hinged Shallow Arch Under Central Concentrated Load.

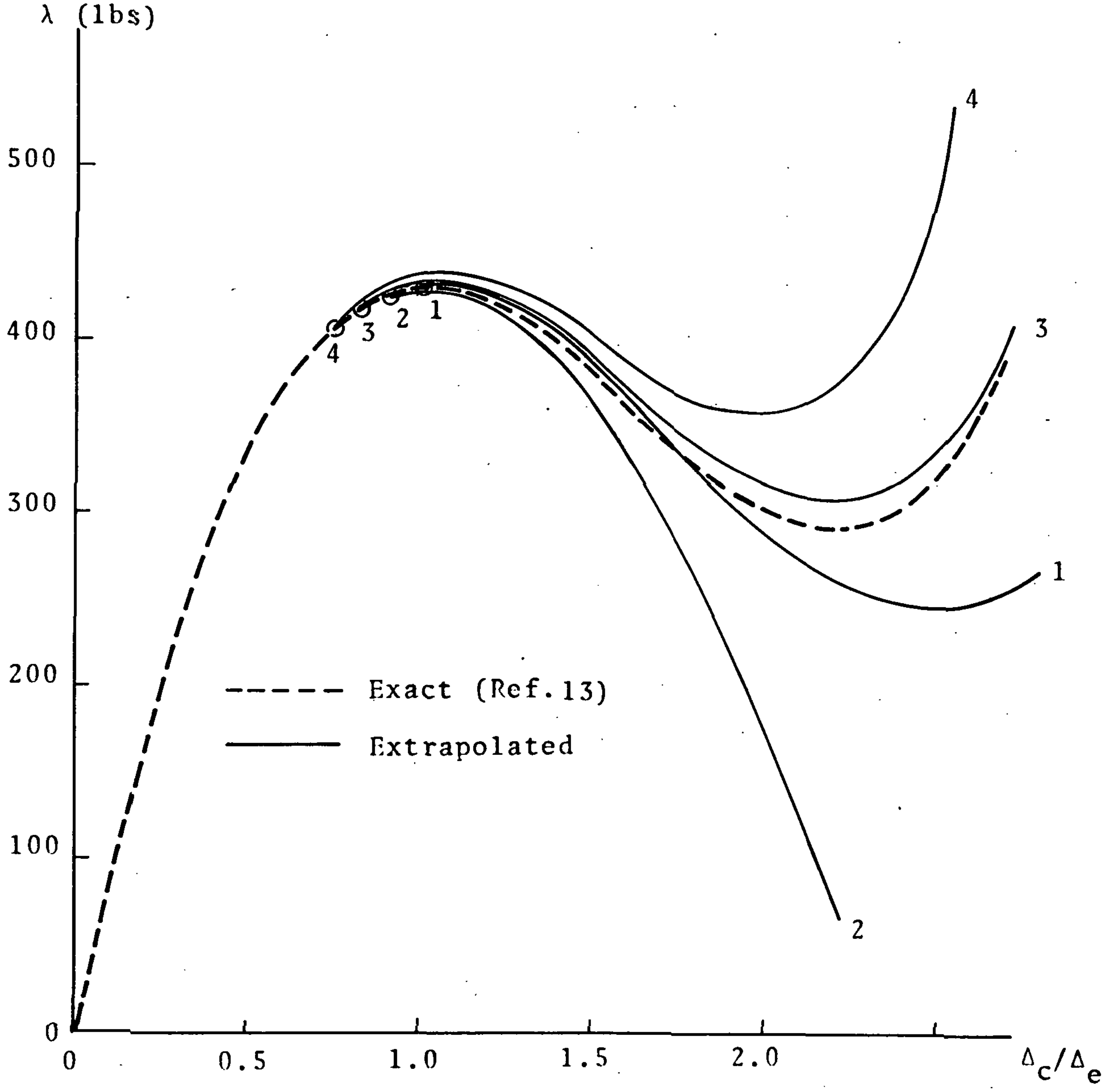

8. Extrapolations Beyond Limit Point of Arch Load-Displacement Behavior.

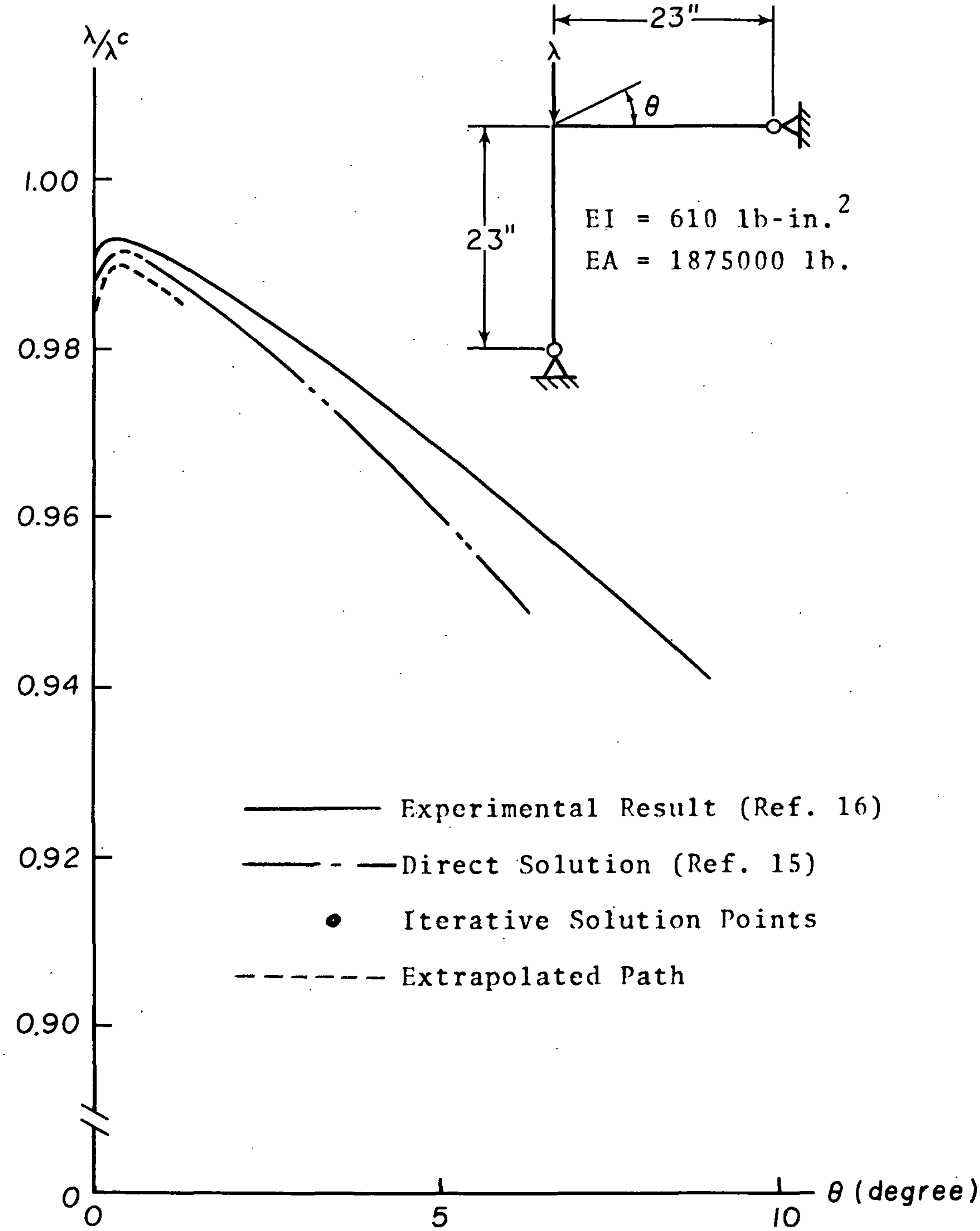

9. Load-Displacement Behavior of Knee-Frame Under Point Load.

"The aeronautical and space activities of the United States shall be conducted so as to contribute . . . to the expansion of human knowledge of phenomena in the atmosphere and space. The Administration shall provide for the widest practicable and appropriate dissemination of information concerning its activities and the results thereof."

—NATIONAL AERONAUTICS AND SPACE ACT OF 1958

NASA SCIENTIFIC AND TECHNICAL PUBLICATIONS

TECHNICAL REPORTS: Scientific and technical information considered important, complete, and a lasting contribution to existing knowledge.

TECHNICAL NOTES: Information less broad in scope but nevertheless of importance as a contribution to existing knowledge.

TECHNICAL MEMORANDUMS: Information receiving limited distribution because of preliminary data, security classification, or other reasons.

CONTRACTOR REPORTS: Scientific and technical information generated under a NASA contract or grant and considered an important contribution to existing knowledge.

TECHNICAL TRANSLATIONS: Information published in a foreign language considered to merit NASA distribution in English.

SPECIAL PUBLICATIONS: Information derived from or of value to NASA activities. Publications include conference proceedings, monographs, data compilations, handbooks, sourcebooks, and special bibliographies.

TECHNOLOGY UTILIZATION PUBLICATIONS: Information on technology used by NASA that may be of particular interest in commercial and other non-aerospace applications. Publications include Tech Briefs, Technology Utilization Reports and Technology Surveys.

Details on the availability of these publications may be obtained from:

SCIENTIFIC AND TECHNICAL INFORMATION OFFICE

NATIONAL AERONAUTICS AND SPACE ADMINISTRATION

Washington, D.C. 20546